Journal Pre-proof

Fluorescent immunoliposomal nanovesicles for rapid multi-well immuno-biosensing of histamine in fish samples

Vivek K. Bajpai, CheolWoo Oh, Imran Khan, Yuvaraj Haldorai, Sonu Gandhi, Hoomin Lee, Xinjie Song, Myunghee Kim, Ashutosh Upadhyay, Lei Chen, Yun Suk Huh, Young-Kyu Han, Shruti Shukla

PII: S0045-6535(19)32644-X

DOI: https://doi.org/10.1016/j.chemosphere.2019.125404

Reference: CHEM 125404

To appear in: *ECSN*

Received Date: 5 August 2019

Revised Date: 11 November 2019

Accepted Date: 18 November 2019

Please cite this article as: Bajpai, V.K., Oh, C., Khan, I., Haldorai, Y., Gandhi, S., Lee, H., Song, X., Kim, M., Upadhyay, A., Chen, L., Huh, Y.S., Han, Y.-K., Shukla, S., Fluorescent immunoliposomal nanovesicles for rapid multi-well immuno-biosensing of histamine in fish samples, *Chemosphere* (2019), doi: https://doi.org/10.1016/j.chemosphere.2019.125404.

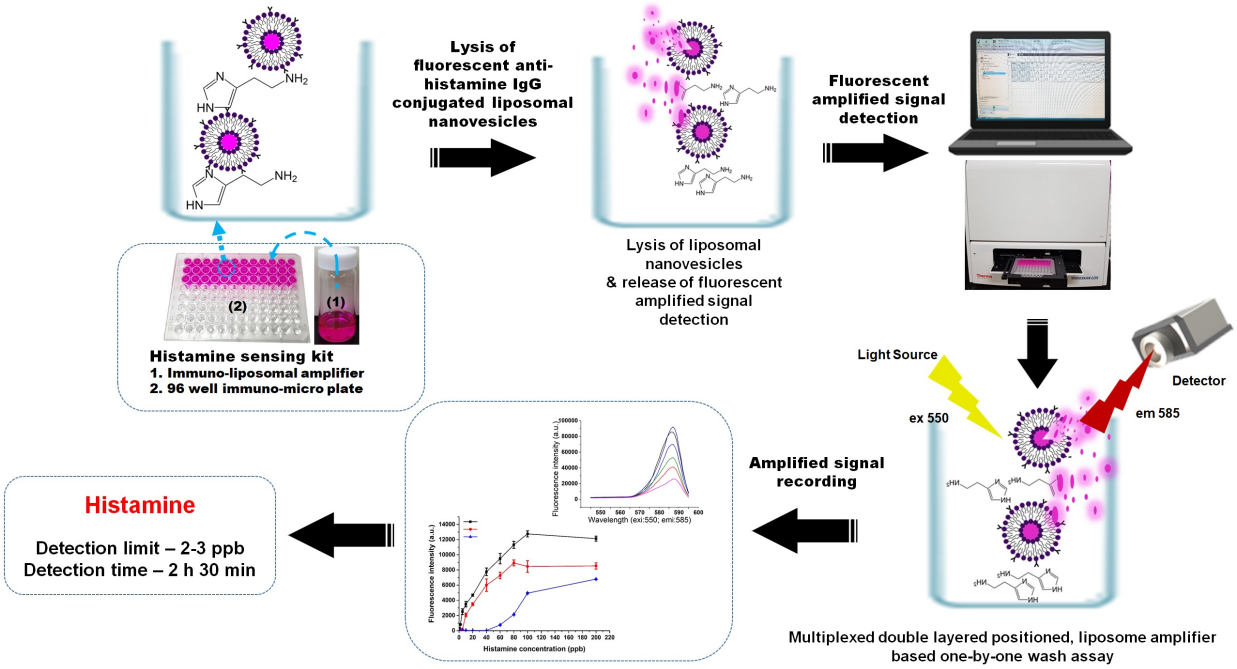

Fluorescent immunoliposomal nanovesicles for rapid multi-well immuno-biosensing of histamine in fish samples

Vivek K. Bajpai [a,$], CheolWoo Oh [b,$], Imran Khan [b], Yuvaraj Haldorai [c], Sonu Gandhi [d], Hoomin Lee [b], Xinjie Song [e], Myunghee Kim [e], Ashutosh Upadhyay [f], Lei Chen [g,*], Yun Suk Huh [b,*], Young-Kyu Han [a,*], Shruti Shukla [h,*]

[a] *Department of Energy and Materials Engineering, Dongguk University-Seoul, 30 Pildong-ro 1-gil, Seoul 04620, Republic of Korea*

[b] *Department of Biological Engineering, Biohybrid Systems Research Center (BSRC), Inha University, 100 Inha-ro, Nam-gu, Incheon 22212, Republic of Korea*

[c] *Department of Nanoscience and Technology, Bharathiar University, Coimbatore-641046, Tamil Nadu, India*

[d] *DBT-National Institute of Animal Biotechnology (DBT-NIAB), Hyderabad 500032, Telangana, India*

[e] *Department of Food Science and Technology, Yeungnam University, Gyeongsang-si, Republic of Korea*

[f] *Department of Food Science and Technology, National Institute of Food Technology Entrepreneurship and Management (NIFTEM), Sonipat, Haryana 131028, India*

[g] *College of Food Science, Fujian Agriculture and Forestry University, Fuzhou, Fujian 350002, China*

[h] *Department of Food Science and Technology, National Institute of Food Technology Entrepreneurship and Management (NIFTEM), Sonipat, Haryana 131028, India*

[$] **Equally contributed**

Running head: Immunoliposomal nanovesicles for time resolved detection of histamine

Corresponding authors:

Dr. Yun Suk Huh; E-mail: yunsuk.huh@inha.ac.kr; **Dr. Lei Chen;** E-mail: chenlei841114@hotmail.com; **Dr. Young-Kyu Han**; E-mail: ykenergy@dongguk.edu; **Dr. Shruti Shukla**: E-mail: shruti.shukla15@yahoo.com

ABSTRACT

Scombroid poisoning in fish-based and other food products has raised concerns due to toxicity outbreaks and incidences associated with histamine, thus measuring the amount of histamine toxic molecule is considered crucial quality indicator of food safety and human health. In this study, liposome-based measurement of histamine was performed via rupturing mechanism of sulforhodamine B dye encapsulated anti-histamine antibody conjugated liposomal nanovesicles. The immunosensing ability of immuno-liposomal format was assessed by monitoring the fluorescence at excitation/emission wavelength of 550/585 nm. Immuno-liposomal format assays were considered, one based on single wash procedure (Method 1), which had a detection limit of 10 ppb and quantification limit 15-80 ppb. While Method 2 based on one-by-one wash procedure had a detection limit of 2–3 ppb and quantification limit 8.5 ppb–200 ppm that required 2 h 30 min to perform. In view of better quantification limit, Method 2 was chosen for further tests required to validate its applicability in real samples. The feasibility of Method 2 was reconfirmed in fresh mackerel fish, and canned fish (tuna and salmon) with a similar detection limits but with low amplified fluorescence signals and sufficient levels of histamine recovery from fresh mackerel (73.50-99.98%), canned tuna (79.08–103.74%) and salmon (74.56–99.02%). The specificity and method accuracy were expressed as % CV in the range 5.34%-8.48%. Overall, the developed multi-well sensing system (Method 2) showed satisfactory specificity, cost effectiveness, rapidity, and stability for monitoring histamine toxicity as a practical food diagnostic device.

Keywords: Double layered; Liposome immunosensor, Signal amplifiers, Fluorescence quenching, Histamine toxicity

1. Introduction

Since 1960s optical detection systems have been used as a powerful tool to allow light propagation with a minimum loss for use in sensor development strategies. Similarly, nowadays, fluorescence technology has emerged as a mean of sensitivity enhancer with reduced matrix effects, making it applicable for biosensing purposes (Chang et al., 2016). Food scientists are concerned about several issues related to the contamination of protein-rich food products by endogenous bioactive amines as chemical messengers in biological systems (Lin et al., 2018). Nowadays, histamine contamination of food is common and considered a serious human health and food safety issue, hence, fabrication of fluorescence assay for real time monitoring of food toxicants, such as histamine, has attracted huge attention. Histamine is mainly formed in protein-rich food matrices by certain microorganisms that produce histidine decarboxylase, which catalyzes the conversion of free histidine to histamine (EFSA, 2011). Given that fish consumption is variable, a serving size of 250 g was considered reasonable to establish a maximum level of histamine in fish of 200 mg/kg (FAO, 2012), whereas the United States Food Drug Administration (USFDA) set the histamine threshold limit at 50 mg/kg (FDA, 2011). Hence, the sensitive and selective detection of histamine is of considerable importance from the safety and clinical perspectives and for studies on allergic responses under various pathological conditions (Yan et al., 2014; Yang et al., 2015). Therefore, it is essential to develop sufficiently sensitive and rapid cost effective methods to detect histamine residues for clinical and food diagnosis.

A number of analytical detection methods have been developed for the determination of histamine levels in food products, including reverse-phase high performance liquid chromatography (RP-HPLC), cation-exchange chromatography (CEC), gas chromatography (GC), thin layer chromatography (TLC) (Awan et al., 2008; Lapa-Guimarães and Pickova,

2004) and ELISA based assays (Luo et al., 2014). Although these analytical techniques have provided adequate for detecting a variety of analytes, time-consuming sample processing steps, such as, clean-up, sample derivatization, and the low optical absorbance of histamine in the ultraviolet region are problematic.

To address these problems, biosensors have attracted interest as potential rapid analytical sensing tools as alternatives to traditional enzyme-based detections. Several rapid, one-step electrochemical biosensors based on enzymes or nanozymes (Pérez et al., 2013; Jiang et al., 2015; Veseli et al., 2016; Yadav et al., 2019) have been devised for the sensing of histamine. However, the specificity cannot be ensured for these biosensors as the enzymes used can catalyze histamine and its analogues. Further, several technologies use various nanomaterials in combination with electrochemical and fluorescence detection techniques as signal amplifiers (Ali et al., 2017; Pei et al., 2013; Rusling, 2012; Du et al., 2011). These nanomaterials include gold nanoparticles (Du et al., 2011), quantum dots (Qian et al., 2011), magnetic nanoparticles (Mani et al., 2009), silica nanoparticles (Wu et al., 2009) and carbon nanomaterials (Malhotra et al., 2010), and have ability to enhance the signals while using as nano carriers. Since the significant signal releasing process from various nanocarriers is complicated as some of these require strong acid, base, heat and sonication treatments, which might have adverse effect on biological molecules, such as enzymes, antibody and antigenic targets (Zhao et al., 2015).

Thus, there is a need for more sensitive/specific signal amplifier tools, and this need might be met by antibody-based immunosensing detection strategies employing fluorescent nanoparticles. Although a few fluorescence-based detection devices have been used for food samples safety analysis (Liu et al., 2016; Yang et al., 2017; Kaur et al,. 2018; Chauhan et al., 2018), no fluorescence-nano-sensing-based multi-well method has yet been devised that uses layer by layer arranged fluorescence dye encapsulated immuno-liposome nanovesicles for

amplifying histamine toxin or other biogenic amines detecting signals in food matrices via antigen-antibody capturing, liposome vesicle rupturing and signal release. Hence, we afforded to incorporate with a liposomal fluorescence-amplifier to determine the feasibility of a new multi-well biosensing platform for histamine toxin in food matrices.

Lumen of liposomes encapsulates any biological molecules with the help of liposomal aqueous core capacity and phospholipid head groups of polar nature that can play an important role for the improvement of signal amplification, and can be used as multifunctional vesicles (Edwards and Baeumner, 2006). It has been reported that liposomes exhibited better performance for advanced biosensors as compared to other signal amplification materials (Edwards and Baeumner, 2006). Also, immunosensors based on antigen-antibody interactions exhibit superior characteristics as compared to enzyme-based immunoassays due to their high sensitivities and excellent specificities (Zhang et al., 2016). Moreover, liposome-based assays where markers (antibody) and fluorescent dyes are encapsulated in the liposomes as detectable molecules, provide instant signal enhancement after lysis mechanism as compared to enzyme-based immunoassays which show time and concentration dependent signal enhancement, thus limiting the sensitivities and the speed of analysis. Specifically, the liposome-based assay proposed in this study requires comparatively lesser washing and incubation steps for antigen-antibody reactions as well as eliminates the separate reaction of secondary antibody and reaction with HRP-tagged signal generating molecules. The total assay time of the proposed method is only 2 h and 30 min as compared to ELISA-based methods which require various processing steps such as coating (12 h incubation), washing with buffer solution (5-10 min), blocking (2 h incubation) re-washing with buffer solution (5-10 min), IgG addition (1 h incubation) followed by washing with buffer solution (require 5-10 min), addition of labeled enzyme (1 h incubation) followed by washing with buffer solution (5-10 min), enzyme substrate reaction (30 min incubation) and

addition of stop solution (NaOH) followed by absorbance measurement. A few additional factors also make the immunoliposome-based assay (after antibody conjugation) favorable as compared to other ELISA-based histamine detection assays due to their (1) instant fluorescence signal enhancement ability after the lysis mechanism, (2) cost effectiveness, and (3) an alternate over other fluorescence materials.

Thus far, only very few liposome-based rapid and multi-well detection methods have been developed for histamine toxin. Therefore, the current study was undertaken to construct Sulforhodamine B dye encapsulated phospholipid bilayers with anti-histamine antibody conjugated liposomal nanovesicles as an amplifier, positioned in a 2 layered format [single well one wash format (Method 1) and one by one wash format (Method 2) that unites for strong fluorescence signal, after rupturing the constructed lipid bilayer. The developed multi-well biosensing method (Method 2) exhibited excellent properties of fluorescence excitation on particular wavelength and signal amplification via tagged antibody molecule on the outer surface of fluorescent liposomal nanovesicles. In order to confirm the novelty of the developed method (Method 2), sensitive detection of histamine in buffer medium and fish samples, was validated to achieve the goal of the study by developing a rapid detection method that can overcome the drawbacks associated with Method 1 and conventional analytical methods, including HPLC and other liposomal sensing methods. The detection sensitivity and applicability of fluorescent anti-histamine IgG conjugated liposomal nanovesicles (anti-His-LNs)-based biosensing system was compared in real food matrix with a conventional HPLC method to validate its simplicity, precision, rapidity, repeatability and straightforwardness.

2. Materials and methods

2.1. Chemicals and reagents

Putrescine dihydrochloride (PUT), histamine dihydrochloride (HIS), cadaverine dihydrochloride (CAD), 2-phenylethylamine (PHE), tryptamine hydrochloride (TRP), spermidine trihydrochloride (SPD), spermine tetrahydrochloride (SPM), tyramine hydrochloride (TYR), N-(2-hydroxyethyl) piperazine-N-2-ethanesulfonic acid (HEPES), sodium azide, sodium chloride, *n*-Octyl-*β*-D-glucopyranoside (OG), methanol, acetone, cholesterol, sucrose, Sepharose CL-4B, triethylamine, dansyl chloride, potassium phosphate monobasic, ethylene diamine tetra acetic acid (EDTA), potassium phosphate dibasic, dimethyl sulfoxide (DMSO) and amino acids, including histidine, glycine, alanine, lysine, glutamic acid and arginine were obtained from Sigma, USA. Sulforhodamine B was purchased from Molecular Probes, USA. Ammonium hydroxide, sodium hydroxide, perchloric acid, and sodium hydrogen carbonate were purchased from Junsei Chemicals, Japan. 1,2-Dipalmitoyl-sn-glycero-3-phosphocholine (DPPC), 1,2-dipalmitoyl-sn-glycero-3-[phospho-rac-(1-glycerol)] (DPPG), and 1,2-dipalmitoyl-sn-glycero-3-phosphoethanolamine (DPPE) were procured from Avanti Polar Lipids, USA. N-[κ-maleimidoundecanoyloxy] sulfosuccinamide (sulfo-KMUS), *N*-Succinimidyl-*s*-acetylthioacetate (SATA), and hydroxylamine hydrochloride were obtained from Pierce Products, USA. Monoclonal anti-histamine antibody (anti-histamine IgG) (cat#MBS358003; 1 mg/mL) was purchased from MyBioSource, USA. Immunoplates (96 well amine binding polystyrene surface) were purchased from Thermo Scientific (USA).

2.2. Synthesis of Sulforhodamine B-encapsulated liposome nanovesicles

Liposome nanovesicles were prepared using a reverse-phase evaporation method we previously described with a few modifications in our earlier methodology. In brief, a lipid mixture (40.3 µmol: DPPC, 4.2 µmol: DPPG, and 40.9 µmol: cholesterol) was used to form a phospholipid bilayer, and a fluorescent dye Sulforhodamine B at higher concentration (150 mM) was selected to make fluorescent liposome nanovesicles, as we previously described (Shukla et al., 2016). Non-encapsulated dye or trace of organic solvent was removed from the liposome preparation by gel-filtration on a Sephadex G-50 column (1.5×18 cm) at room temperature. Detailed methodology for synthesizing Sulforhodamine B-encapsulated liposome nanovesicles has been given in the Section 1 of the supplementary information.

2.3. Surface functionalization of fluorescent liposome nanovesicles and conjugation of anti-histamine IgG to develop immunosensor

Step I. Derivatization of anti-histamine IgG with maleimide functional group

Fluorescent anti-histamine conjugated liposomal nanovesicles (anti-His-LNs) as nanobiosensors were prepared as previously described with some modification [28]. Briefly, 0.1 mg of anti-histamine IgG was dissolved in 1 mL of 0.05 M potassium phosphate buffer containing 1 mM of EDTA and 0.01% sodium azide (pH 7.4). A sulfo-KMUS solution was prepared by dissolving 3 mg of sulfo-KMUS in 0.15 mL of solvent mixture of DMSO: MeOH (2:1, v/v). Then, a 2.25 µl of sulfo-KMUS solution was then added to 1 mL of this anti-histamine IgG solution (0.1 mg/mL) and incubated on a shaker at room temperature for 3 h [29, 30]. Once the antibody (0.1 mg of anti-histamine IgG) derivatized with the maleimide group, was dialyzed overnight with 0.02 M HEPES buffer (0.15 M NaCl, 0.01% sodium azide), and sucrose was added to maintain its osmolarity as 427 m osmol/L. Importantly, to

maintain the proper stability of Sulforhodamine B-encapsulated liposomes, all buffers used in the liposome preparation were adjusted to relatively a little higher osmolarity so as to prevent the osmotic pressure-related swelling.

Step II. Removal of acetylthioacetate group from Sulforhodamine B-encapsulated liposome nanovesicles

The *N*-succinimidyl-*s*-acetylthioacetate (SATA) was used during the first step of liposome synthesis to prepare DPPE-ATA complex by mixing DPPE (7.2 µmol) and SATA (14.3 µmol) with 1 mL of 0.7% trimethylamine. After incorporation of lipid constituents into liposome bilayer, final obtained Sulforhodamine B-encapsulated liposome nanovesicles may still have some amounts of acetylthioacetate group moieties from SATA, which should be removed prior to further processing reaction (Kindly refer to supplementary information section for more information).

The total volume of Sulforhodamine B-encapsulated liposome solution was measured as it may differ lot-to-lot. 0.5 M of hydroxylamine hydrochloride was prepared in 0.1 M HEPES solution containing 25 mM EDTA (pH 7.4) and then added into Sulforhodamine B-encapsulated liposome solution in a working ratio of 1:10 (1 mL of Sulforhodamine B-encapsulated liposome solution; 0.1 mL of 0.5 M hydroxylamine hydrochloride solution) followed by flushing the flask under nitrogen for 1 min. The reaction process of deacetylation was allowed to occur at room temperature at 70 rpm shaker for at least 2 h.

Step III. Conjugation of maleimide-derivatized anti-histamine IgG to Sulforhodamine B-encapsulated liposome nanovesicles

Conjugation of maleimide-derivatized anti-histamine IgG and fluorescent liposome nanovesicles (210 µL) was performed by adjusting the liposome solution mixture to pH 7.0 using 0.5 M HEPES buffer (to make same pH as required for –SH group ethylmaleimide quenching, 0.02 M Tris buffer; pH 7.0), added with maleimide-derivatized anti-histamine IgG solution (0.1 mg/mL of anti-histamine IgG prepared in Step I), and flushing under nitrogen gas for 1 min. The reaction was allowed to proceed on a shaker at room temperature for 4 h and then incubated at 4ºC overnight. To quench unreacted –SH groups, 100 mM of ethylmaleimide dissolved in 0.02 M Tris buffer containing 0.15 M NaCl, 0.01% NaN_3, and 0.07 M sucrose; pH 7.0 was added to the immunoliposomes reaction mixture; the osmolarity of this buffer solution (421 m osmol/L) was maintained with 0.07 M sucrose using an osmometer (Shukla et al., 2016). Anti-histamine IgG-tagged liposome nanovesicles were separated from unreacted SH-derivatized anti-histamine IgG using a Sepharose CL-4B column equilibrated with 0.02 M Tris buffer (0.15 M NaCl, 0.01% NaN_3, pH 7.0) containing 0.07 M sucrose. The desired fraction of anti-histamine IgG-tagged liposome nanovesicles was collected and the solution was dialyzed (in 0.02 M Tris buffer) overnight at 4 ºC in the dark for achieving to improve its stability. The confirmation of free antibody released during elution from Sepharose CL-4B column was analyzed in different fractions of elute buffer via the Bradford method using rabbit IgG as a standard.

After this, the measured volume of anti-histamine IgG-tagged liposome nanovesicles was then treated with dropwise addition of 2% BSA solution (in 0.01 M phosphate buffer), followed by 30 min incubation at 4ºC to block non-specific binding (Kim et al., 2018). This pre-blocking step was preferable in this study than our previously reported method (Shukla et al., 2016) due to lesser chances of non-specific binding that could be originated from contamination of antibody-conjugated liposome nanovesicles. As illustrated in Fig. 1, phospholipids and cholesterol moieties were used to construct a nano-sized Sulforhodamine

B dye encapsulated lipid bilayer (liposome) and conjugated with anti-histamine IgG to form immunoliposome nanovesicles after fractionation and purification using Sephadex and Sepharose gel columns.

2.4. Characterization of fluorescent anti-histamine IgG conjugated liposomal nanovesicles

2.4.1. Morphology, size, and stability

Liposome nanovesicles morphologies were observed using a JEOL 2100F high-resolution TEM. Average diameters, polydispersity indices (PDI), and zeta potentials of liposome nanovesicles were measured by dynamic light scattering (DLS) using a Zetasizer Nano ZS particle analyzer (Malvern Instruments Ltd., Worcestershire, UK) at room temperature. Intensities of liposomal suspensions were adequately diluted with 0.02 M Tris-buffered saline (TBS pH 7.0) prior to taking measurements. The PDI and zeta potentials of fluorescent liposome nanovesicles were also used as measures of particle homogeneity and stability.

2.4.2. Confirmation of Sulforhodamine B *encapsulation in liposomal lipid bilayers*

Lipid and phospholipid molecules can encapsulate Sulforhodamine B, a self-quenching signaling molecule at higher concentrations leading to formation of Sulforhodamine B-encapsulated liposome nanovesicles; Sulforhodamine B-encapsulation efficiency was determined by measuring increases in fluorescence intensity after rupturing lipid bilayers. In brief, 150 mM Sulforhodamine B-encapsulated liposome nanovesicles were treated with a solution of *n*-Octyl-*β*-D-glucopyranoside (OG) (30 mM) and few other ionic and non-ionic detergent reagents such as Tween 20, Tween 80, Triton X-100, and sodium dodecyl sulfate. After the lysis, the fluorescence intensities of released Sulforhodamine B

from encapsulated liposome nanovesicles were recorded at 550 and 585 nm as excitation and emission wavelengths, respectively, and for control, 0.01 M HEPES buffer (pH 7.0) was used.

2.4.3. Confirmation for free anti-histamine IgG release via Sepharose CL-4B column

Anti-histamine IgG-tagged liposome nanovesicles were separated from free anti-histamine IgG using a Sepharose CL-4B column. The confirmation of free antibody released during elution from Sepharose CL-4B column was analyzed by collecting different fractions of elute buffer after different time intervals and released free antibody concentration was measured via the Bradford method using rabbit IgG as a standard (Shukla et al., 2011).

2.5. Concept for detection assay format and sensitivity for histamine detection

The developed assay functions on the immuno-capturing-based fluorescence controlled detection efficiency of liposome nanovesicles, which act as signal amplifiers. The detection signal capacity of a liposome particle is directly proportional to its size, as described previously (Shukla et al., 2016). The basic concept of the present assay is based on fluorescence measurement before and after rupturing of liposomes followed by leakage of encapsulated SRB dye from the liposome vesicles and finally enhanced fluorescence signals are generated as compared to the fluorescence measurement without rupturing. In the present assay method, we simplified and specified the arrangement of liposomal vesicles for generating strong signals, better sensitivity, reduced washing, single well reaction, reduced cost, and instant signal generation by using developed immunoliposome vesicles rather than an enzyme-based assay with fluorescence detections. The overall setup for anti-His-LNs-based biosensing is demonstrated in Fig. 2. The liposomal nanovesicles containing Sulforhodamine B amplifiers exhibit strong absorption at 500 nm and high fluorescence at

550 and 585 nm as excitation and emission wavelengths, respectively (data not shown), hence these parameters were introduced into our setup to allow the detection of fluorescence signals. Thus ability of liposome nanovesicles to act as immunosensor for histamine sensing was assessed by monitoring the change of fluorescence at an excitation wavelength of 550 nm and emission wavelength of 585 nm.

In the present study, an arrangement strategy of fluorescent anti-His-LNs was adopted to enhance the detection efficiency of the developed assay format. In brief, at first, a stock solution of anti-histamine IgG-tagged liposome nanovesicles (anti-His-LNs) was diluted with 0.01 M Tris buffered saline (TBS) containing 0.04 M sucrose at ratios of 1:2, 1:5, 1:10 or 1:50 to obtain suitable fluorescence signals in terms of intensities. The 1:10 ratio was deemed optimal and used throughout the remainder of the study. Disruption of the phospholipid bilayer of liposomal nanovesicles was induced by adding detergent. The release of Sulforhodamine B was then detected by analyzing increases and/or decreases in fluorescence intensities. Two assay formats based on two layered anti-His-LNs (anti-His-LNs were mixed with histamine antigen to form immunocomplex, the procedure was done in 2 layers) were constructed in an effort to shorten and simplify the detection procedure. Schematics of the both methods are presented in Figures 2A, B and C.

Method 1 involves a single well one wash procedure, in which 100 µL solution of various concentrations of histamine (1, 5, 10, 20, 40, 60, 80, 100 or 200 ppb in 0.01 M phosphate buffer) was added in micro-wells of 96 well amine binding polystyrene surface immunoplate, followed by incubation at 37 ºC for 15 min and then addition of 50 µL of anti-His-LNs and incubated for 15 min at 37 ºC. These amine binding polystyrene surface 96 microwell plates allow the strong adhesion of proteins and antigenic molecules, including histamine. In brief, these plates were pre-activated via maleic anhydride which allows strong attachment of amine-containing molecules to microplate wells for using in binding assays.

Here, our target molecule is a type of biogenic amine (histamine) having $–NH_2$ functional group, therefore, similar binding approach is strongly suitable in these plates.

Then, similarly the mixture of 100 µL of histamine solution and 50 µL anti-His-LNs as a secondary layer was added to each well followed by similar incubation procedure to allow the formation of immunocomplex (Fig. 2A). Wells were then washed with 0.01 M phosphate buffer and 250 µL of 30 mM OG was added to lyse the liposome nanovesicles. Histamine bounded Sulforhodamine B encapsulated liposome nanovesicles were then lysed and released. At final step, 200 µL of supernatant solution was transferred in to the new well, and fluorescence signals of Sulforhodamine B, generated after lysis, were measured at 550 and 585 nm as excitation and emission wavelengths, respectively.

On the other hand, another detection assay procedure for Method 2 involved a one-by-one wash procedure (Fig. 2B). Briefly, at first 100 µL of histamine solution of various concentrations (1, 5, 10, 20, 40, 60, 80, 100 or 200 ppb and higher concentrations 0.5-200 ppm in 0.01M phosphate buffer) was coated onto micro-wells of 96 well surface immunoplate by incubating the microplate for 30 min at 37° C. Wells were then washed with 0.01 M phosphate buffer (3 times), and then 50 µL of anti-His-LNs were added, and wells were incubated at 37 °C for 30 min to initiate the immunogenic reaction. The wells were again washed with 0.01 M phosphate buffer (3 times). Similarly, a second layer of assay format was constructed by adding 100 µL of histamine solution and 50 µL of antibody-tagged liposome nanoparticles followed by incubation at 37 °C for 30 min after each addition. Then, the micro-wells were again washed three times with 0.01 M phosphate buffer and then encapsulated Sulforhodamine B molecules (in anti-His-LNs) were released by adding 250 µL of 30 mM OG. Finally, 200 µL of lysed liposome solution (supernatant) was transferred in to the new well (to avoiding false interference of any down settled aggregated immunocomplex and errors due to bubbles originated after addition of OG), and signal generation in terms of

fluorescence intensity was measured at an excitation wavelength of 550 nm and emission wavelength of 585 nm. The fluorescence intensities of samples and blank were measured as positive and negative values, respectively. The detection results were evaluated for positive/negative (P/N) values, where P/N >2 is considered as a positive result which means histamine is present at detectable level, and P/N < 2 is considered as a negative result which means histamine is either not present or at a very low concentration.

The method for using 2 layers of liposomal vesicles in sensitive detection of enterotoxic *Staphylococcus aureus* was originated from Yin and Wen (2017). To prove better detection performance, a single layered immuno-liposomal assay format was constructed and compared with current 2 layered immuno-liposomal format. Single layer for immunosensing was formed similarly by adding 100 µL of histamine solution to coat onto micro-wells of 96 well amine binding polystyrene surface immunoplate by incubating the microplate for 30 min at 37° C followed by 3 times washing (using 0.01M phosphate buffer). After which 50 µL solution of anti-His-LNs was added to micro-wells followed by incubation at 37 °C for 30 min. Wells were then washed with 0.01 M phosphate buffer and fluorescence signals were recorder after the lysis of anti-His-LNs by adding 250 µL of 30 mM OG. For measuring the fluorescence signals (at excitation and emission wavelengths of 550 and 585 nm, respectively), only 200 µL of lysed liposome solution was transferred to the new wells (Fig. 2C).

2.6. Interference test

The developed one-by-one assay (Method 2) was tested for its specificity against histamine. Solutions of eight other endogenous standard biogenic amines (HIS, TRP, SPD, PHE, CAD, PUT, TYR, and SPM) were prepared at 10 and 100 ppb concentrations, whereas

their commonly representing corresponding free amino acids (histidine, glycine, alanine, lysine, glutamic acid and arginine) were prepared separately at higher concentration levels (100 ppb) for interference test. The mixture of HIS was prepared at 10 ppb while other interfering amines and free amino acids were prepared at 10×excess concentrations and tested using the above-described analytical procedure. All assay sets were performed in six replicates and % CV values were calculated.

2.7. Applicability of developed detection assay in contaminated fish, meat and ready to eat salad products

Histamine is a heat stable amine and is unaffected by high range of temperatures and imposes a great challenge in terms of public health and trade by possessing scombroid fish poisoning. To confirm the applicability of the proposed sensing via Method 2, the content of histamine in fresh mackerel fish, canned tuna and salmon fish, ground red meat and ready to eat salad samples was detected using spiked recovery method. All the fresh samples were transferred in hygienic conditions to the laboratory and then exposed under UV for 20-30 min to avoid any further microbial contaminations and further tested using commercially available histamine detection kit (Neogen-veratox for quantification limit 2 ppm) as well as via currently developed method for the detection of lower levels of histamine (in ppb) in order to confirm the absence of histamine in each set of the sample detection analysis and then spiked with histamine at different concentration levels.

All samples (5 g) after confirming the absence of histamine were homogenized (high speed) in 45 mL of 0.01 M phosphate buffer (pH 7.0) and homogenates were then spiked with different concentrations of histamine (1, 5, 10, 20, 40, 60, 80, 100 or 200 ppb) and final volumes made up to 50 mL. After vigorous vortexing, samples were centrifuged at 10,000

rpm for 10 min, 1 mL aliquots of supernatant were collected and diluted at 1:10 to reduce matrix effects. In continuations of assay procedure as ascribed in earlier section for method 2, collected supernatant from histamine contaminated real samples was coated onto micro-wells of 96 well amine binding polystyrene surface immunoplate by incubating the microplate for 30 min at 37° C. These specific immunoplates have the high adhesion and easy attachment capacity of amine binding polystyrene surfaces for histamine antigen present in the samples. Three independent sets of spiked samples were prepared at each concentration for statistical purposes.

2.8. Assay validations

The detection procedure was validated via calibration curve and evaluation of the range of linearity, limit of detection (LOD), and limit of quantification (LOQ). The linear response of histamine was determined in the concentrations, which led to the correlation factor $R^2 > 0.99$. LOD and LOQ were re-calculated using the standard equations LOD = X0 + 3SD and LOQ = X0 + 5SD, respectively, where X0 was the average response of the blank samples, and SD referred to the standard deviation for n = 6.

3. Results and discussion

3.1. Preparation and characterization of liposome nanovesicles

Sulforhodamine B-encapsulated liposome nanovesicles were developed using a reverse-phase method as previously described (Shukla et al., 2016) with minor modifications. In brief, liposome nanovesicles were filtered through 0.8 and 0.4 µm polycarbonate filters in

order to achieve uniform size distributions (Fig. 1D), which were measured by dynamic light scattering at 209.2 nm with 100% intensity and 0.965 intercept value (Fig. S1). Average volume of single liposome nanoparticle calculated using average size of mixed liposome vesicles is presented in Table S1. On the basis of the average size determined via dynamic light scattering, it could be possible to calculate the average outer volume of single liposome vesicle as 4.71×10^{-12} µL and inner volume entrapped (by assumption 4 nm lipid bilayer thickness) as 4.18×10^{-15} µL. The Sulforhodamine B content inside the liposome was assumed as equal to Sulforhodamine B concentration used during the liposome preparation (150 mM), and other characteristics such as amount of Sulforhodamine B per liposome (6.28×10^{-13} µmol), number of Sulforhodamine B molecules per liposome (3.78×10^{5}) were calculated by comparing the fluorescence of lysed liposomes to that of standard Sulforhodamine B solution. Amount of lipid / liposome and number of lipid molecules per liposomes were calculated considering the outer surface area= $4\pi r^2$ with the assumption that only 50% of total lipid molecules are present in liposome vesicle. Similarly, anti-histamine IgG molecules tagged per liposomal vesicles were calculated by assuming that only 0.4% IgG was conjugated that resulted in 2200 molecules of anti-histamine IgG on the surface of each liposomal vesicle. Prior to antibody conjugation, the concentration of developed liposomes was calculated by assuming that the Sulforhodamine B concentration inside liposomes was 150 mM. All calculations were dependent on Sulforhodamine B standard curve and calculated as encapsulated Sulforhodamine B concentrations after lysis and measured via fluorescence intensity (at an excitation wavelength of 550 nm and emission wavelength of 585 nm) for the total released SRB concentration, as a result, which was calculated as 8 µmol/mL of liposome solution. Based on the information given in Table S1, we calculated the µmol concentration of SRB/each particle of liposome as 6.28×10^{-13}. Therefore, the concentration of liposome (particles/mL) was approximately 1.27×10^{13} particles/ mL. All the calculations were

designed on the bases of our earlier reported protocols (Shin and Kim, 2008).

Previous studies have shown that fluorescence detection signal capacity of a liposome nanoparticle is dependent to its particle size (Shin and Kim, 2008). Based on this information, we assumed that as the size of the surface area of a liposome particle increased the binding affinities of antibody molecules to its surface was enhanced. Thus, we sought to prepare liposome nanovesicles with high surface areas to enhance surface antibody binding. TEM observations confirmed 190–200 nm nanovesicles were spherical (Fig. 3A). Also, Shin and Kim (2008) reported that as the size of the liposome increased, higher fluorescence signals were obtained owing to a higher number of Sulforhodamine B molecules encapsulated in the liposome. Overall, as the liposome particle size increased, the detection signal increased.

Zeta potential and polydispersity index (PDI) are important parameters that reflect the stabilities of nano-systems, and for Sulforhodamine B-encapsulated liposome nanovesicles as determined by DLS their values were −42 ± 7.72 mV, and 0.191, respectively, which confirmed interaction between Sulforhodamine B molecules and negatively charged phospholipids (Table S1). Liposomes prepared with lower PDIs (< 1) are considered monodisperse liposome vesicles, and have excellent stabilities (Shukla et al., 2011). The magnitude of the zeta potential indicates the potential stability of the colloidal system. High surface charges cause particles to repel each other, and thus, increase solution stability. Li et al. (2016) reported similar results for liposome nanovesicles developed for targeted drug delivery.

3.2. Confirmation of Sulforhodamine B encapsulation in liposomal lipid bilayers

Sulforhodamine B was successfully encapsulated in liposome nanovesicles and

served as a strong fluorescent sensing material. To confirm the encapsulation efficiency of liposomes, results were confirmed based on the measurements of the fluorescence intensity of Sulforhodamine B-encapsulated liposomes before and after lysis. In addition, we also tested the abilities of a series of ionic and non-ionic detergents (Tween 20, Tween 80, Triton X-100, sodium dodecyl sulfate, and OG) to rupture the membranes of Sulforhodamine B-encapsulated liposomes (Fig. 3B). OG at a concentration of 30 mM was found to most effectively rupture lipid membrane as determined by transmission electron morphological views (Fig. 3C) and Sulforhodamine B fluorescence intensities (Fig. 3D).

Fluorescence intensities of lysed and non-lysed liposomal nanovesicles rely on the de-quenching of putatively self-quenched Sulforhodamine B (Ho et al., 2007). In order to determine the concentration dependency of Sulforhodamine B release from liposomes nanovesicles and generation of fluorescent signals by lysis of liposomal nanovesicles. Liposome nanovesicles at different dilutions ($1:10^3$, $1:10^4$, $1:10^5$, and $1:10^6$) were treated with 30 mM of OG as a strong detergent, and fluorescence intensity signals were measured at excitation and emission wavelengths of 550 and 585 nm, respectively. We found that 30 mM OG dose-dependently induced Sulforhodamine B release, and thus, was chosen for further tests (Fig. 3D). Overall our results showed Sulforhodamine B was well encapsulated by liposomal vesicles, which exhibited only weak fluorescence intensity, but strong fluorescence intensity after lysis, indicative of fluorescent dye leakage from vesicles (Saez et al., 1982).

Further, after conjugation of anti-histamine IgG to Sulforhodamine B-encapsulated liposome nanovesicles, the free antibodies were removed following the purification step via Sepharose CL-4B column. The confirmation of released free antibody was validated using different interval fractions of elute buffer by the Bradford method using rabbit IgG as a standard. During conjugation, initial concentration of anti-histamine IgG was 0.1 mg/mL while 0.021 mg/mL of free antibody release was observed during purification of anti-

histamine IgG from different fractions of buffer via Sepharose CL-4B column (Table S3), confirming that the free antibody was easily removed when fractioned via Sepharose CL-4B column. The optimization of anti-histamine useful amount for the conjugation with liposomal nanovesicles was tested with various concentrations of anti-histamine IgG antibody to achieve its significant bounding efficiency confirmed via Bradford test. Finally, 0.1 mg/mL concentration was confirmed as the useful amount of anti-histamine IgG to form immunoconjugate (Table S2). The experiment was allowed to perform in several lots during the synthesis procedure.

3.3. Design and detection sensitivity of developed assay

Under optimized conditions, immunosensor assay formats (Methods 1 and 2) constructed in this study based on the immunoliposome nanovesicles were applied to detect different concentrations of histamine in a buffer system (Fig. 4A and 3B). Both methods produced dual layer liposome-based immunocomplex with the requirement of 200 µL of analyte (histamine) and 100 µL of anti-His-LNs. Method 1 was involved a single well one wash procedure, in which a second layer of immunocomplex was formed with anti-His-LNs and was mixed together with single step washing followed by fluorescence measurements by the release of Sulforhodamine B contents. On the other hand, Method 2 involved the multiple washing and incubation steps typical of ELISA into a one-by-one procedures as described in the Experimental section in which first analyte (histamine antigen) was coated with proper incubation time followed by 3 times washing and then the first layer of anti-His-LNs was constructed. After proper incubation period, the attached immunocomplex was washed and again allowed to construct a second layer of analyte and anti-His-LNs followed by washing. Method 1 and 2 resulted in LINs that exhibited concentration-dependent fluorescence

intensities (Fig. 4A and 4B). Lower concentration of histamine allowed the formation of antigen (histamine)–antibody (anti-His-LNs) complex only in a few amount, and large amount of anti-His-LNs remained unbounded, which can be easily washed off, and after lysis reaction, resulting in a lower range of fluorescence intensity which was observed in an increasing manner as the concentration of histamine increased (Fig. 4A and 4B).

Detection limits were defined as average fluorescence intensities of blank samples plus-minus three standard deviations (Hochel and Skvor, 2009). In brief, according to the equation: LOD = xb1 + 3sb1, where xb1 is average blank signal and sb1 is blank standard deviation. The detection limit of histamine for Method 1 was found to be 10 ppb and only 1 h 15 min was required to obtain signals (Fig. 4A). While, Method 2 (one by one wash) had a detection limit of 2–3 ppb but 2 h 30 min was required to obtain signals (Fig. 4B). The detection limit of Method 2 was preferred, presumably due to stronger analyte to anti-His-LNs binding due to the longer reaction time. In Method 1, the “prozone effect” was observed at a histamine concentration of 80 ppb, and this may have been due to competitive reactions between anti-His-LNs and higher number of histamine molecules which can be considered as a saturation point (Fig. 4A). On the other hand, Method 2 showed minute reduction in fluorescence signals at a histamine concentration of 200 ppb (Fig. 4B); however, on an increment of higher histamine concentrations (0.5 to 200 ppm), fluorescent signals again increased drastically and no saturation or “prozone effect” was observed (Fig. S4), possibly due to the use of multiple washes in between the arrangements of anti-His-LNs complex offering a heterogeneous assay design (Vaidya et al., 1988).

Based on these results, although Method 1 could be implemented more easily and quickly because it did not require multiple steps of Method 2, we adopted Method 2 because it had a lower detection limit (2–3 ppb) and a quantification limits in a wider range (8.5 ppb–200 ppm) than Method 1 (15–80 ppb). We believe that the two layered anti-His-LNs based

sensing format (Method 2) exhibited good bio-specificity and sensitivity- the emitted fluorescence was acquired from the detection of anti-histamine IgG-conjugated liposomal amplifiers that formed strong layers of immuno-complexes with the target analyte and the immuno-liposomal complex. This may be attributed to the inherited nature of the anti-His-LNs as an immunosensor which specifically captured the analyte molecule. Moreover, the appropriate blocking strategy also prevented non-specific binding between the detection surface and the target antibody molecules or liposomal amplifiers (Chang et al., 2016).

In a previous study, Shukla et al. (2012) used liposomes in a single layer format for the detection of *Salmonella* bacterium. Here, we compared a single layered format involving multiple washing stages similar with Method 2 (two layered format) using the same amount of histamine (200 µL) and of liposome nanovesicles (100 µL) and measured detection sensitivities (Fig. 2B). We found the detection limit of histamine in single layered format was 60 ppb and that signals were detected in 1 h 30 min (Fig. 4C). This outcoming demonstrated an immense interest in achieving better detection sensitivities by approaching a two layered format of liposome nanovesicle-based diagnostic system. Finally, we compared the analytical performance of Method 2 with other diagnostic methods developed for histamine detection (Table 1). Method comparisons demonstrated that the sensor developed in this study has a wider linear range and a lower detection limit, and does not require the complex handling steps of previously reported sensors.

To check storage stability, fluorescence intensities of synthesized Sulforhodamine B-encapsulated liposome nanovesicles were measured after storage at 4 ºC for 6 and 12 months. Significant changes in fluorescence intensity were observed after 3 months and after 12 months of storage fluorescence intensities were much reduced (Fig. S2). Therefore, in order to achieve long term stability and avoid damage of fluorescent liposome nanovesicles, we recommend the conjugation of anti-histamine IgG to fluorescent liposome nanovesicles

should be performed promptly after synthesis. Therefore, after conjugation of liposomal nanovesicles with anti-histamine IgG (immunoliposomal nanovesicle), we evaluated the stability with storage at 4 ºC for 0 month to 20 months, and observed that the stability of immunoliposomal nanovesicles in terms of fluorescence intensity was not reduced until 12 months, which proves their significant stable shelf-life with sufficient encapsulation of SRB dye. However, a drastic reduction in the fluorescence intensity was noted after 12 and 14 months storage under the same conditions.

3.4. Specificity of the developed assay formats

In order to measure the specificity of Method 2, cross-reactivity was examined versus 8 other biogenic amines (HIS, PUT, PHE, SPM, CAD, TRP, SPD, and TYR) that belong to same group of amine contaminants in food products. All the examinations were performed under the experimental conditions described in subsection: 2.5. Positive and negative tests were conducted using fluorescence intensities and P/N values. P/N values of many immunoassays provide an important means of determining positive and negative test results (Saez et al., 1982). The P/N value of histamine was 7.49 ± 0.2 (>2), whereas for the other biogenic amines tested, P/N values were all <2, which indicated the absence of cross reactivity with other amine contaminants. The P/N value of spermidine was 2.4 ± 0.1, indicating slight interference (Fig. 5a). This might be due to close chemical interaction of spermidine moieties or a few uncovered binding sites present in anti-His-LNs. The specificity of the developed anti-His-LNs-based assay (Method 2) is probably determined by the specificity of the antibody used (Dong et al., 2017).

The selectivity was also investigated with the correspondent free amino acids found mostly in fish, meat and vegetables as histidine, glycine, alanine, lysine, glutamic acid and

arginine, account for major proportion of the total amino acid contents. The histidine amino acid is the main interfering factor for histamine determination because the % presence of free amino acids in meat and fish products is lesser than 1%. Fig. 5b shows the fluorescence intensity response of these free amino acids along with histamine and found the peak fluorescence intensity of histamine was minimum 3 times larger at $1/10^{th}$ concentration of other tested free amino acids, approved for no interfering with other structural analogs. Also when a mixture of all free amino acids (100 ppb) mixed with histamine at 10 ppb, fluorescence intensity of histamine was slightly reduced as compare to single histamine (10 ppb) but was analyzed statistically different ($p < 0.05$), confirming acceptable specificity of the proposed sensing. Few other electrocatalytic electrodes based sensing methods were found to be affected by interfering analogs including histidine free amino acid (Wang et al., 2017; Gajjala and Palathedath, 2018).

3.5. Applicability of the developed assay using real fish and meat samples

In order to assess the applicability of the developed anti-His-LNs-based assay (Method 2), fish food products including fresh mackerel fish and canned tuna/salmon fish samples were artificially spiked with corresponding histamine concentrations. The histamine detection limit was found to be same as in buffer medium (2–3 ppb), but fluorescence signals were slightly reduced (Fig. 6), indicating slight matrix effects, presumably due to high protein, fat, or omega fatty acid contents present in fish samples (Omanovic-Miklicanin and Valzacchi, 2017). Further, average recoveries were also tested with detectable concentrations observed from fresh mackerel 73.50% to 99.98%, canned tuna 79.08% to 103.74% and 74.56% to 99.02% from canned salmon, respectively. The precision and accuracy of each test set were expressed as % CVs ranging from 1.48% to 6.86% (Table 2). These analytical figures (% CV)

were consistent with the results of other reported detection approaches, indicating that the method was reliable for the analysis of real samples (Hu et al., 2017; Taghdisi et al., 2016).

Solution obtained (after spiking of histamine into real food samples) was diluted in the ratio of 1:10 to reduce matrix effects following the USFDA guidelines and coated onto the amine group binding polystyrene 96 well immunoplates. At this stages along with histamine, a few other proteins present in food samples might also be coated onto the surfaces of immunoplate. However, the developed assay had no interfering effect on the histamine specific fluorescence signal generation, thus confirming the specificity of currently developed anti-His-LNs based assay (Method 2).

Moreover, histamine detection with good recovery was also confirmed in few other relevant food matrices such as ground red meat and ready to eat salad. The results of an acceptable value of % histamine recoveries were found as 106.43% and 99.00% in ground red meat and ready to eat salad, respectively are provided in Table S5. The total assay time of the developed assay setup for all the samples was noted as 2 h 30 min, including coating, blocking and washing procedures. This assay setup favors that multiple samples (96 samples at one time) can be handled within the same time limit. These results revealed a good sensing applicability of the developed one-by-one anti-His-LNs-based assay (Method 2) in a multi-well biosensing system for a variety of food matrices without having any recovery loss and no demand for sophisticated purification methods, such as extraction-based liquid chromatography methods.

3.6. Method comparison with conventional HPLC technique and liposome-based immunomagnetic separation assay

Although several analytical detection methods, including HPLC, GC, RP-HPLC, and

TLC have been reported earlier (Awan et al., 2008; Lapa-Guimarães and Pickova, 2004) for the detection of histamine, all these methods require sample pre-treatment step, derivatization prior to sample injection, and able to analyze only single sample at a time. However, the sensing method developed in this study does not have any requirement of pre-treatment, sample derivatization and able to analyze multiple samples at the same time. Further, to approve the novelty, accuracy and practical applicability of the developed anti-His-LNs-based assay (Method 2), fish food products, including fresh mackerel and canned tuna/salmon fish samples were tested for measuring the histamine content by the proposed method and high performance liquid chromatography (HPLC) method.

To confirm the sensitivity, rapidity, and straightforwardness of the sample pre-treatment procedure without using expensive reagents and derivatizing reagents, results were verified using a conventional HPLC method. We previously found, histamine had to be derivatized with dansyl or benzoyl chloride for HPLC detection (Shukla et al., 2011; Shukla et al., 2014), as fish samples spiked with different biogenic amines at different concentrations, including histamine, could not be analyzed without derivatization. Therefore, same fish samples were extracted with 0.4 M perchloric acid and derivatized with dansyl chloride followed by HPLC analyses. The results from HPLC chromatograms confirmed lower histamine recovery rates than currently developed anti-His-LNs-based method (Table S4, Fig. S3). HPLC techniques for the determination of several hazardous biogenic amines, including histamine, require sample extraction and derivatization (2–3 h), and a sample run time of 30 min. The assay procedure developed in the present study does not require any pre-treatment or sample derivatization step, and was able to detect histamine in multiple samples (at least 96 samples) directly within 2 h 30 min.

Furthermore, histamine concentrations of < 1 ppm could not be easily detected in a variety of food matrices by HPLC technique, which is its major limitation versus nano-based

detection techniques. Erim (2013) reported that HPLC technique can be used to quantify a single biogenic amine in a sample, and by HPLC, limit of detection of 0.02 ppm has been reported for histamine in fish products. Pradenas et al. (2016) confirmed and validated an improved HPLC technique in different food matrices for the detection of histamine with a limit of detection ranging from 0.5–20 ppm.

In addition, we have also compared the novelty, and better detection limits of anti-His-LNs-based method (Method 2) with other liposome-based immunomagnetic concentration and separation assay (IMS) (Shukla et al., 2016). As a result, although the total assay time was similar (2 h 30 min) as observed for the anti-His-LNs-based method, in histamine buffer medium the detection limit was found as 10-20 ppb with quantification limit of 10-50 ppb (Fig. 7). The practical applicability of liposome-based immunomagnetic concentration and separation assay was also compared in real fish food sample spiked with different concentrations of histamine. As a result, although direct detection without sample pre-treatment was confirmed, the detection and quantification limits were very poor as 20 ppb and 20-50 ppb, respectively than currently developed anti-His-LNs-based assay (Method 2), which indicates that the developed assay (Method 2) could be used efficiently for the routine analysis of histamine in real food samples than other similar detection methods.

4. Conclusions

A fluorescence quenching immunosensing format was developed to measure the concentration of histamine toxin in contaminated fish samples. The developed liposome amplified sensing assay (Method 2) shown preferable detection limit of 2–3 ppb with a wide range for quantification limit (8.5 ppb –200 ppm). Validation of the developed assay procedure (Method 2) was confirmed by histamine detection in artificially contaminated real

fish samples where a similar detection limit (2-3 ppb) was achieved within 2 h 30 min of total assay time for multiple samples (96 samples at one time), including coating, blocking and washing procedures without use of extraction and derivatization steps than that of conventional analytical detection methods such as HPLC. The histamine recovery rates form contaminated fish samples were in the range of 73.50%-103.74% whereas repeatability results as % CV were in the range of 5.34%-8.48%. In summary, the liposome-based detection assay developed in this study is simple, rapid, and cost effective, and does not require any extra pre-treatment steps. Moreover, it has great potential in a wide range of universal diagnostic applications to determine toxin analytes in real fish samples, including other similar foods.

Author contributions

The manuscript was written through contributions of all authors. All authors have given approval to the final version of the manuscript.

Declaration of interests

None.

Acknowledgments

We acknowledge financial support from the Basic Science Research Program through the National Research Foundation of Korea (NRF) funded by the Ministry of Science, ICT & Future Planning (2016R1A2B4013374 and 2014R1A5A1009799).

References

Ali, M., Ramirez, P., Duznovic, I., Nasir, S., Mafe, S., Ensinger W., 2017. Label-free histamine detection with nanofluidic diodes through metal ion displacement mechanism. Colloids Surf. B Biointerfaces 150, 201–208.

Awan, M.A., Fleet, I., Paul Thomas, C.L., 2008. Determination of biogenic diamines with a vaporisation derivatisation approach using solid-phase microextraction gas chromatography–mass spectrometry. Food Chem. 111, 462–468.

Chang, Y-.F., Fu, C., Chen, Y-.T., Jou, F-.J., Chen, C-.C., Chou, C., Ho, J.A., 2016. Use of liposomal amplifiers in total internal reflection fluorescence fiber-optic biosensors for protein detection. Biosens. Bioelectron. 77, 1201–1207.

Chauhan, N., Gupta, S., Avasthi, D.K., Adelung, R., Mishra, Y.K., Jain, U., 2018. Zinc oxide tetrapods based biohybrid interface for voltammetric sensing of *Helicobacter pylori*. ACS Appl. Mater. Interfaces 10, 30631–30639.

Dong, X.X., Yang, J.Y., Luo, L., Zhang, Y.F., Mao, C., Suna, Y.M., Lei, H.T., Shen, Y.D., Beierd, R.C., Xu, Z.L., 2017. Portable amperometric immunosensor for histamine detection using Prussian blue-chitosan-gold nanoparticle nanocomposite films. Biosens. Bioelectron. 98, 305–309.

Du, D., Wang, J., Wang, L.M., Lu, D.L., Smith, J.N., Timchalk, C., Lin, Y.H., 2011. Magnetic electrochemical sensing platform for biomonitoring of exposure to organophosphorus pesticides and nerve agents based on simultaneous measurement of total enzyme amount and enzyme activity. Anal. Chem. 83, 3770–3777.

Edwards, K.A., Baeumner, A.J., 2006. Analysis of liposomes. Talanta 68, 1421–1431.

EFSA, 2011. European Food Safety Association, Scientific opinion on risk based control of

biogenic amine formation in fermented foods. EFSA J. 9, 2393–2487.

Erim, F.B., 2013. Recent analytical approaches to the analysis of biogenic amines in food samples. Trends Anal. Chem. 52, 239–247.

FAO, 2012. Food and Agriculture Organization, Codex Alimentarius Commission. Joint FAO/WHO Food Standard Programme. Codex Committee on Fish and Fishery Products, 32 session Discussion paper histamine, 1–14.

FDA, 2011. Food and Drug Administration, Fish and fisheries products hazards and controls guide (4th Ed.), Washington, DC: Office of Seafood, Food and Drug Administration.

Gajjala, R.K.R., Palathedath, S.K., 2018. Cu@Pd core-shell nanostructures for highly sensitive and selective amperometric analysis of histamine. Biosens. Bioelectron. 102, 242–246.

Gajjala, R.K.R., Palathedath, S.K., 2018. Cu@Pd core-shell nanostructures for highly sensitive and selective amperometric analysis of histamine. Biosens. Bioelectron. 102, 242–246.

Gustiananda, M., Andreoni, A., Tabares, L.C., Tepper, A.W.J.W., Fortunato, L., Aartsma, T.J., Canters, G.W., 2012. Sensitive detection of histamine using fluorescently labeled oxido-reductases. Biosens. Bioelectron. 31, 419–425.

Ho, J.A., Wu, L.C., Huang, M.R., Lin, Y.J., Baeumner, A.J., Durst, R.A., 2007. Application of ganglioside-sensitized liposomes in a flow injection immunoanalytical system for the determination of cholera toxin. Anal. Chem. 79, 246–250.

Hochel, I., Skvor, J., 2009. Characterisation of antibodies for the immunochemical detection of *Enterobacter sakazakii*. Czech J. Food Sci. 27, 66–74.

Hu, S., Ouyang, W., Guo, L., Lin, Z., Jiang, X., Qiu, B., Chen, G., 2017. Facile synthesis of Fe_3O_4/g-C3N4/HKUST-1 composites as a novel biosensor platform for ochratoxin A. Biosens. Bioelectron. 92, 718–723.

Janc˘I, T., Valinger, D., Kljusuric´, J.G., Mikac, L., Vidac˘ek, S., Ivanda, M., 2017. Determination of histamine in fish by Surface Enhanced Raman Spectroscopy using silver colloid SERS substrates. Food Chem. 224, 48–54

Jiang, S., Peng, Y., Ning, B., Bai, J., Liu, Y., Zhang, N., Gao, Z., 2015. Surface plasmon resonance sensor based on molecularly imprinted polymer film for detection of histamine. Sens. Actuat. B-Chem. 221, 15–21.

Kaur, N., Kaur, M., Chopra, S., Singh, J., Kuwar, A., Singh, N., 2018. Fe(III) conjugated fluorescent organic nanoparticles for ratiometric detection of tyramine in aqueous medium: A novel method to determine food quality. Food Chem. 245, 1257–1261.

Kim, J., Oh, S.Y., Shukla, S., Hong, S.B., Heo, N.S., Bajpai, V.K., Chun, H.S., Jo, C.H., Choi, B.G., Huh, Y.S., Han, Y.K., 2018. Heteroassembled gold nanoparticles with sandwich-immunoassay LSPR chip format for rapid and sensitive detection of hepatitis B virus surface antigen (HBsAg). Biosens. Bioelectron. 107, 118–122.

Lapa-Guimarães, J., Pickova, J., 2004. New solvent systems for thin-layer chromatographic determination of nine biogenic amines in fish and squid. J. Chromatogr. A 1045, 223–232.

Li, J., Guo, C., Feng, F., Fan, A., Dai, Y., Li, N., Zhao, D., Chen, X., Lu, Y., 2016. Co-delivery of docetaxel and palmitoyl ascorbate by liposome for enhanced synergistic antitumor efficacy. Sci. Rep. 6, e38787.

Lin, Y.T., Chen, C.H., Lin, M.S., 2018. Enzyme-free amperometric method for rapid determination of histamine by using surface oxide regeneration behavior of copper electrode. Sens. Actuat. B-Chem. 246, 2838–2843.

Liu, J., Chen, Y., Wang, W., Feng, J., Liang, M., Ma, S., Chen, X., 2016. Switch-On" fluorescent sensing of ascorbic acid in food samples based on carbon quantum dots–MnO_2 probe. J. Agric. Food Chem. 64 (2016) 371–380.

Luo, L., Xu, Z.L., Yang, J.Y., Xiao, Z.L., Li, Y.J., Beier, R.C., Sun, Y.M., Lei, H.T., Wang, H.,

Shen, Y.D., 2014. Synthesis of novel haptens and development of an enzyme-linked immunosorbent assay for quantification of histamine in foods. J. Agric. Food Chem. 62, 12299−12308.

Luo, L., Yang, J.Y., Xiao, Z.L., Zeng, D.P., Li, Y.J., Shen, Y.D., Sun, Y.M., Lei, H.T., Wang, H., Xu, Z.L., 2015. A sensitivity-enhanced heterologous immunochromatographic assay based on a monoclonal antibody for the rapid detection of histamine in saury samples. RSC Adv. 5, e78833.

Malhotra, R., Patel, V., Vaque, J.P., Gutkind, J.S., Rusling, J.F., 2010. Ultrasensitive electrochemical immunosensor for oral cancer biomarker IL-6 using carbon nanotube forest electrodes and multilabel amplification. Anal. Chem. 82, 3118–3123.

Mani, V., Chikkaveeraiah, B.V., Patel, V., Gutkind, J.S., Rusling, J.F., 2009. Ultrasensitive immunosensor for cancer biomarker proteins using gold nanoparticle film electrodes and multienzyme-particle amplification. ACS Nano 3, 585–594.

Mattsson, L., Jungmann, C., Lieberzeit, P.A., Preininger, C., 2017. Modified carbon black as label in a colorimetric on-chip immunoassay for histamine. Sens. Actuat. B-Chem. 246, 1092–1099.

Moyano, A., Salvador, M., Martínez-García, J.C., Socoliuc, V., Vékás, L., Peddis, D., Alvarez, M.A., Fernández, M., Rivas, M., Blanco-López, M.C., 2019. Magnetic immunochromatographic test for histamine detection in wine. Anal. Bioanal. Chem. 411, 6615–6624.

Omanovic-Miklicanin, E., Valzacchi, S., 2017. Development of new chemiluminescence biosensors for determination of biogenic amines in meat. Food Chem. 235, 98–103.

Pei, X., Zhang, B., Tang, J., Liu, B., Lai, W., Tang, D., 2013. Sandwich-type immunosensors and immunoassays exploiting nanostructure labels: A review. Anal. Chim. Acta 758, 1–18.

Pérez, S., Bartrolí, J., Fàbregas, E., 2013. Amperometric biosensor for the determination of histamine in fish samples. Food Chem. 141, 4066–4072.

Pradenas, J., Galarce-Bustos, O., Henríquez-Aedo, K., Mundaca-Uribe, R., Aranda, M., 2016. Occurrence of biogenic amines in beers from Chilean market. Food Control 70, 138–144.

Qian, J., Dai, H.C., Pan, X.H., Liu, S.Q., 2011. Simultaneous detection of dual proteins using quantum dots coated silica nanoparticles as labels. Biosens. Bioelectron. 28, 314–319.

Rusling, J.F., 2012. Nanomaterials-based electrochemical immunosensors for proteins. Chem. Rec. 12, 164–176.

Saez, R., Alonso, A., Villena, A., Gori, F.M., 1982. Detergent-like properties of polyethyleneglycols in relation to model membranes. FEBS Lett. 137, 323–326.

Shin, J., Kim M., 2008. Development of liposome immunoassay for *Salmonella* spp. using immunomagnetic separation and immunoliposome. J. Microbiol. Biotechnol. 18, 1689–1694.

Shukla, S., Bang, J., Heu, S., Kim, M.H., 2012. Development of immunoliposome-based assay for the detection of *Salmonella* Typhimurium. Eur. Food Res. Technol. 234, 53–59.

Shukla, S., Lee, G., Song, X., Park, S., Kim, M., 2016. Immunoliposome-based immunomagnetic concentration and separation assay for rapid detection of *Cronobacter sakazakii*. Biosens. Bioelectron. 77, 986–994.

Shukla, S., Leem, H., Kim, M., 2011. Development of a liposome-based immunochromatographic strip assay for the detection of *Salmonella*. Anal. Bioanal. Chem. 401, 2581– 2590.

Shukla, S., Park, H.K., Kim, J.K., Kim, M., 2011. Determination of biogenic amines in Japanese *miso* products Food Sci. Biotechnol. 20, 851-854.

Shukla, S., Park, H.K., Lee, J.S., Kim, J.K., Kim, M., 2014. Reduction of biogenic amines and aflatoxins in Doenjang samples fermented with various Meju as starter cultures.

Food Control 42, 181–187.

Taghdisi, S.M., Danesh, N.M., Beheshti, H.R., Ramezani, M., Abnous, K., 2016. A novel fluorescent aptasensor based on gold and silica nanoparticles for the ultrasensitive detection of ochratoxin A. Nanoscale 8, 3439–3446.

Torre, R., Costa-Rama, E., Lopes, P., Nouws, H.P.N., Delerue-Matos, C., 2019. Amperometric enzyme sensor for the rapid determination of histamine. Anal. Methods 11, e1264.

Vaidya, H.C., Wolf, B.A., Garrett, N., Catalona, W.J., Clayman, R.V., Nahm, M.H., 1988. Extremely high values of prostate-specific antigen in patients with adenocarcinoma of the prostate; demonstration of the "hook effect". Clin. Chem. 3, 2175–2177.

Veseli, A., Vasjari, M., Arbneshi, T., Hajrizi, A., Švorc, Ľ., Samphao, A., Kalcher, K., 2016. Electrochemical determination of histamine in fish sauce using heterogeneous carbon electrodes modified with rhenium(IV) oxide. Sens. Actuators B-Chem. 228, 774–781.

Wang, J., Liu, Y., Deng, X., Zhao, N., Ying, X., Ye, B.C., Li, Y., 2017. Hydrogen evolution assisted deposition of a three-dimensional porous nickel film for the electrocatalytic oxidation of histamine. Microchim. Acta 184, 3893–3900.

Wu, Y.F., Chen, C.L., Liu, S.Q., 2009. Enzyme-functionalized silica nanoparticles as sensitive labels in biosensing. Anal. Chem. 81, 1600–1607.

Yadav, S., Nair, S.S., Sai, V.V.R., Satija J., 2019. Nanomaterials based optical and electrochemical sensing of histamine: Progress and perspectives. Food Res. Int. 119, 99–109.

Yan, H., Zhang, X., Hu, W., Ma, J., Hou, W., Zhang, X., 2014. Histamine H3 receptors aggravate cerebral ischaemic injury by histamine-independent mechanisms. Nat. Commun. 5, e3334.

Yang, C., Wang, X., Liu, H., Ge, S., Yu, J., Yan, M., 2017. On–off–on fluorescence sensing of

glutathione in food samples based on a graphitic carbon nitride (g-C_3N_4)–Cu^2+ strategy. New J. Chem. 41, 3374–3379.

Yang, M., Zhang, J., Chen, X., 2015. Competitive electrochemical immunosensor for the detection of histamine based on horseradish peroxidase initiated deposition of insulating film. J. Electroanal. Chem. 736, 88–92.

Ye, W.W., Ding, Y.T., Sun, Y., Tian, F., Yang, M., 2017. A nanoporous alumina membrane based impedance biosensor for histamine detection with magnetic nanoparticles separation and amplification. Procedia Technol. 27, 116 – 117

Yin, H.Y., Wen, H.W., 2017. Dual-labeled PCR-based immunofluorescent assay for the rapid and sensitive detection of enterotoxic *Staphylococcus aureus* using cocktail-sized liposomal nanovesicles as signal enhancer. Food Anal. Methods. 10, 3264–3274.

Zhang, Z., Duan, F., He, L., Peng, D., Yan, F., Wang, M., Zong, W., Jia, C., 2016. Electrochemical clenbuterol immunosensor based on a gold electrode modified with zinc sulfide quantum dots and polyaniline. Microchim. Acta 183, 1089–1097.

Zhao, Y., Du, D., Lin, Y., 2015. Glucose encapsulating liposome for signal amplification for quantitative detection of biomarkers with glucometer readout. Biosens. Bioelectron. 72, 348–354.

Table 1

Comparison of the developed liposomal vesicle-based detection assay for histamine with other detection methods.

Detection base	Mechanism	Limit of detection (LOD)/ Quantification range	Reference
Silver colloid SERS substrate	Surface Enhanced Raman Spectroscopy	Linear range: 0-20 mg/kg	Janc˘I et al., 2017
Cy5 de labeled oxido-reductases	Fluorescent based on quenching by Forster resonance energy transfer	LOD: 13 nM Linear range: 13 nM–25 nM	Gustiananda et al., 2012
Molecularly imprinted polymer film	Surface plasmon resonance sensor	Linear range: 25 µg/L – 1000 µg/L	Jiang et al., 2015
Graphene-based nano composite film with HRP (horse radish peroxidase)	Competitive electrochemical immunosensor	LOD: 0.5 pg/mL Linear range: 1 pg/mL–1 ng/mL	Yang et al., 2015
Nanoporous alumina membranes with magnetic nanoparticles	Impedance based assay	LOD: 1 µM Linear range: 1 µM–40 nM	Ye et al., 2017
Carbon black nanoparticles	Colorimetric based chip immunoassay	0-600 µg/mL	Mattsson et al., 2017
Cu@Pd core shell nanostructures	Chrono amperometry	0.32±0.1 nM	Gajjala and Palathedath, 2018
Commercial ELISA based Kit	Enzyme linked immunosorbent assay	LOD: 2 ppm Linear range: 2.5–40 ppm	Commercial KIT (Neogen Veratox)

Table 1 Continued

Gold nano-particles	Immunochromatographic test strip	LOD: 600 ng/mL (6 mg/kg)	Luo et al., 2015
Screen-printed carbon electrode and the enzyme diamine oxidase	Amperometric sensor	LOD: 0.94 mg/L	Torre et al., 2019
Superparamagnetic particle label	Magnetic immunochromatographic test	LOD: 1.2 mg/L	Moyano et al., 2019
Liposome-based immunomagnetic concentration and separation assay	Fluorescence quenching by Sulforhodamine B dye	LOD: 10–20 ppb Linear range: 15–50 ppb	Compared with current method
Immunoliposomal quenching assay	Fluorescence quenching by Sulforhodamine B dye	LOD: 2–3 ppb Linear range: 8.5 ppb–200 ppm	This work

Table 2

Recovery test results for histamine in fish based food samples (ppb, n = 10).

Fish Food matrices	Spiked concentration (ppb)	Recovered concentration	Average recovery (%)	% CV
Fresh mackerel fish	2	1.47 ± 1.13	73.50 %	4.98
	5	4.13 ± 1.33	82.6 %	3.44
	10	9.16 ± 1.21	91.6 %	3.09
	20	18.78 ± 0.80	93.9 %	3.33
	40	39.10 ± 0.54	97.75 %	2.15
	60	59.99 ± 1.81	99.98 %	2.28
Canned tuna	2	1.58 ± 0.10	79.08 %	6.86
	5	4.47 ± 0.07	89.45 %	1.67
	10	9.47 ± 0.37	94.76 %	4.02
	20	19.21 ± 0.28	96.08 %	1.48
	40	39.20 ± 1.50	98.00 %	3.83
	60	62.24 ± 2.86	103.74 %	4.31
Canned salmon	2	1.52 ± 0.01	76.56 %	4.40
	5	4.25 ± 0.07	85.07 %	1.80
	10	9.36 ± 0.08	93.66 %	1.67
	20	18.93 ± 0.72	94.67 %	3.94
	40	39.47 ± 1.05	98.69 %	2.72
	60	59.41 ± 1.20	99.02 %	2.05

Figure captions

Fig. 1. Preparation of the fluorescent liposomal nanovesicles as signal amplifiers. (A) DPPC, DPPG and cholesterol dissolved in a chloroform/methanol mixture was used to form a thin bilayer film by reverse phase evaporation; (B) Lipid bilayer hydration with aqueous Sulforhodamine B at 45 ºC, (C) Sulforhodamine B-encapsulated in a gel with lipid bilayered vesicles; (D) Liposome nanovesicles were extruded through polycarbonate filters (0.4 and 0.8 µM); (E) Fractionation using Sephadex G-50 gel for collecting Sulforhodamine B-encapsulated fluorescent liposomal nanovesicles; and (F) Conjugation of anti-histamine IgG into fluorescent liposomal nanovesicles with followed by fractionation using Sepharose CL-4B gel for collecting immuno-liposomal nanovesicles with significant fluorescent efficiency.

Fig. 2. Schematic representation for designed multiplexed-optic fluorescent liposomal nanovesicle-based dual layered immuno-biosensing for histamine toxin.

Fig. 3. Characterization of synthesized liposome nanovesicles. (A) Morphological examination of Sulforhodamine B-encapsulated fluorescent liposomal nanovesicles by transmission electron microscopy (TEM); (B) Comparison of using ionic and non-ionic detergents for rupturing the lipid membranes of Sulforhodamine B-encapsulated fluorescent liposomal nanovesicles in terms of released fluorescent Sulforhodamine B dye; (C) TEM images of Sulforhodamine B-encapsulated fluorescent liposomal nanovesicles before (left side image) and after rupturing (right side image) of lipid membrane; and (D) Confirmation of the integrity of 150 mM Sulforhodamine B-encapsulated fluorescent liposomal nanovesicles.

Fig. 4. Sensitivities of the developed double layered positioned anti-His-LNs-based biosensing formats for the detection of histamine. (A) Double layered positioned anti-His-LNs based single well one wash format; (B) Double layered positioned anti-His-LNs based one by one wash format; and (C) Single layered anti-His-LNs-based format. All experiments were conducted three times, and results are presented as means±SDs. The coefficient of variation (% CV) of fluorescence intensity (n=6) was less than 10%.

Fig. 5. Specificity and background interference test of the developed double layered positioned anti-His-LNs-based biosensing for the detection of histamine (A) with coexisting biogenic amines at 10 ppb and 100 ppb concentrations; and (B) with corresponding free amino acids at 100 ppb and histamine at 10 ppb. All experiments were conducted three times, and results are presented as means±SDs. The coefficient of variation (% CV) of fluorescence intensity (n=6) was less than 15%.

Fig. 6. Performance of the immunoliposomal amplified signals based sensing on spiked food matrices (fresh fish, canned fish, ground meat and ready to eat salad) for the detection of histamine. All experiments were conducted three times, and results are presented as means±SDs. The coefficient of variation (% CV) of fluorescence intensity (n=6) was less than 10%.

Fig. 7. Comparison of double layered positioned anti-His-LNs-based biosensing assay with other liposome-based immunomagnetic concentration and separation assay (IMS method) for the detection of histamine.

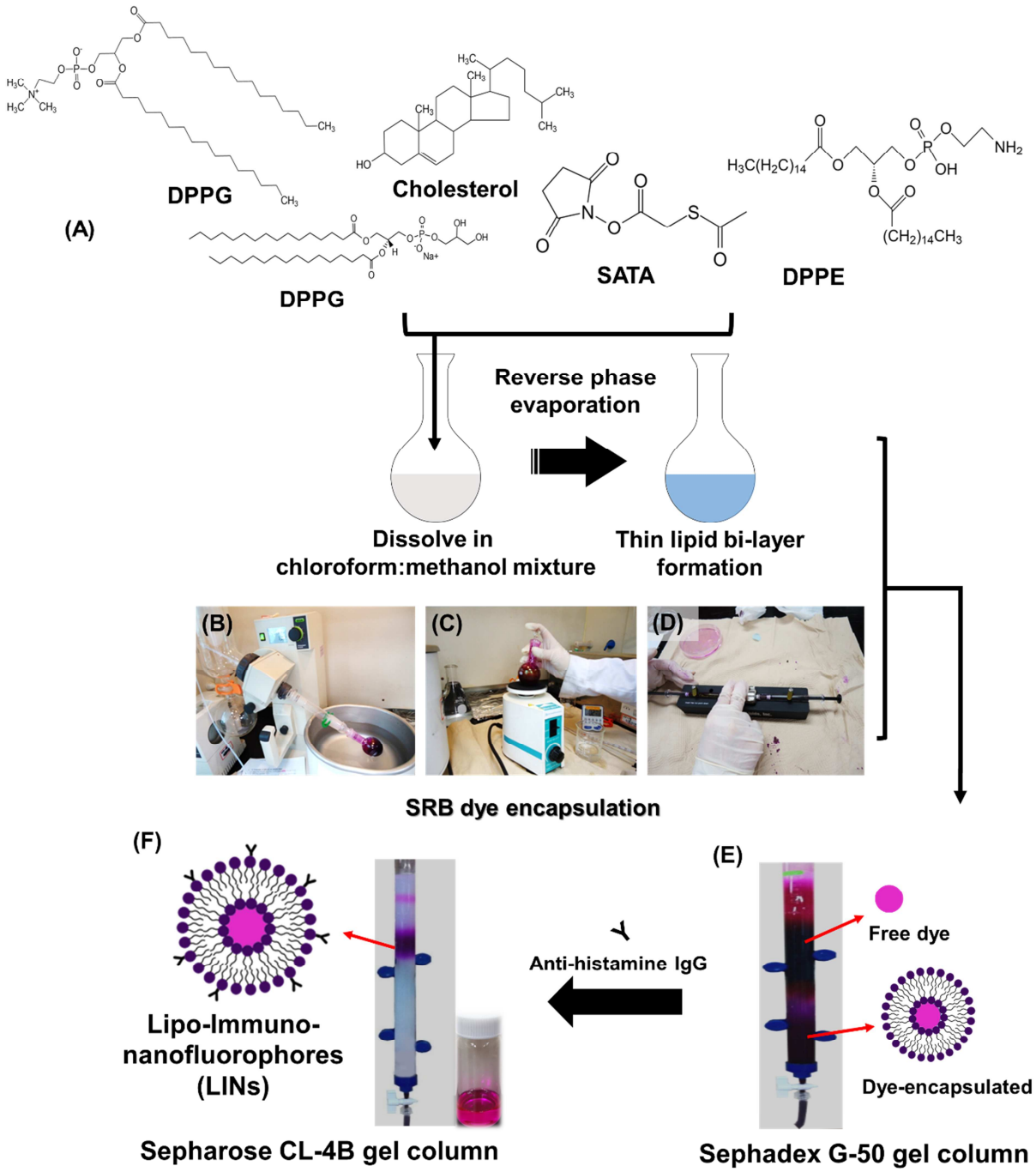
(A)
DPPG
Cholesterol
DPPG
SATA
DPPE
Reverse phase evaporation
Dissolve in chloroform:methanol mixture
Thin lipid bi-layer formation
(B)
(C)
(D)
SRB dye encapsulation
(F)
Lipo-Immuno-nanofluorophores (LINs)
Sepharose CL-4B gel column
Anti-histamine IgG
(E)
Free dye
Dye-encapsulated
Sephadex G-50 gel column

Fig. 1.

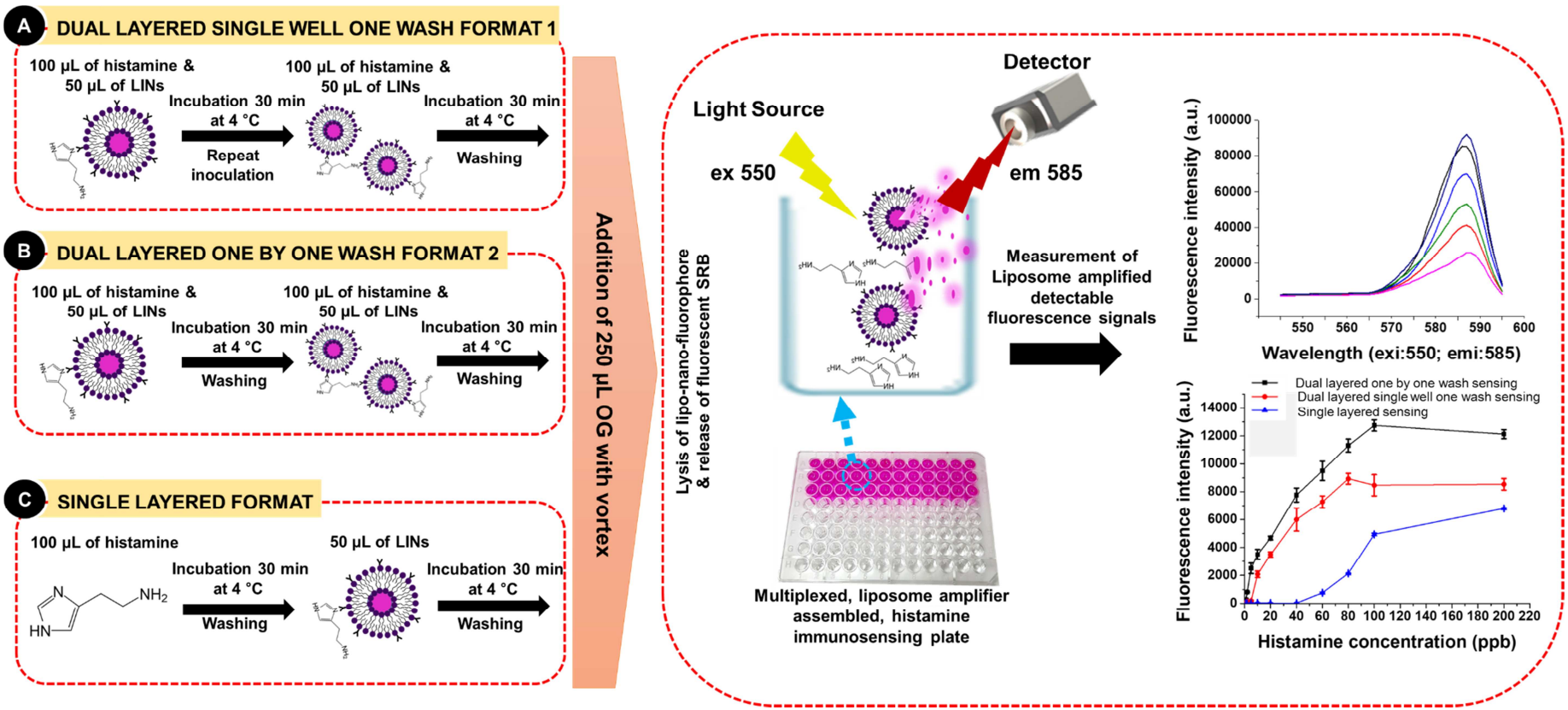
A
DUAL LAYERED SINGLE WELL ONE WASH FORMAT 1
100 µL of histamine & 50 µL of LINs
Incubation 30 min at 4 °C
Repeat inoculation
100 µL of histamine & 50 µL of LINs
Incubation 30 min at 4 °C
Washing
B
DUAL LAYERED ONE BY ONE WASH FORMAT 2
100 µL of histamine & 50 µL of LINs
Incubation 30 min at 4 °C
Washing
100 µL of histamine & 50 µL of LINs
Incubation 30 min at 4 °C
Washing
C
SINGLE LAYERED FORMAT
100 µL of histamine
Incubation 30 min at 4 °C
Washing
50 µL of LINs
Incubation 30 min at 4 °C
Washing
Addition of 250 µL OG with vortex
Light Source
ex 550
Detector
em 585
Lysis of lipo-nano-fluorophore & release of fluorescent SRB
Measurement of Liposome amplified detectable fluorescence signals
Multiplexed, liposome amplifier assembled, histamine immunosensing plate
Fluorescence intensity (a.u.)
Wavelength (exi:550; emi:585)
Dual layered one by one wash sensing
Dual layered single well one wash sensing
Single layered sensing
Fluorescence intensity (a.u.)
Histamine concentration (ppb)

Fig. 2.

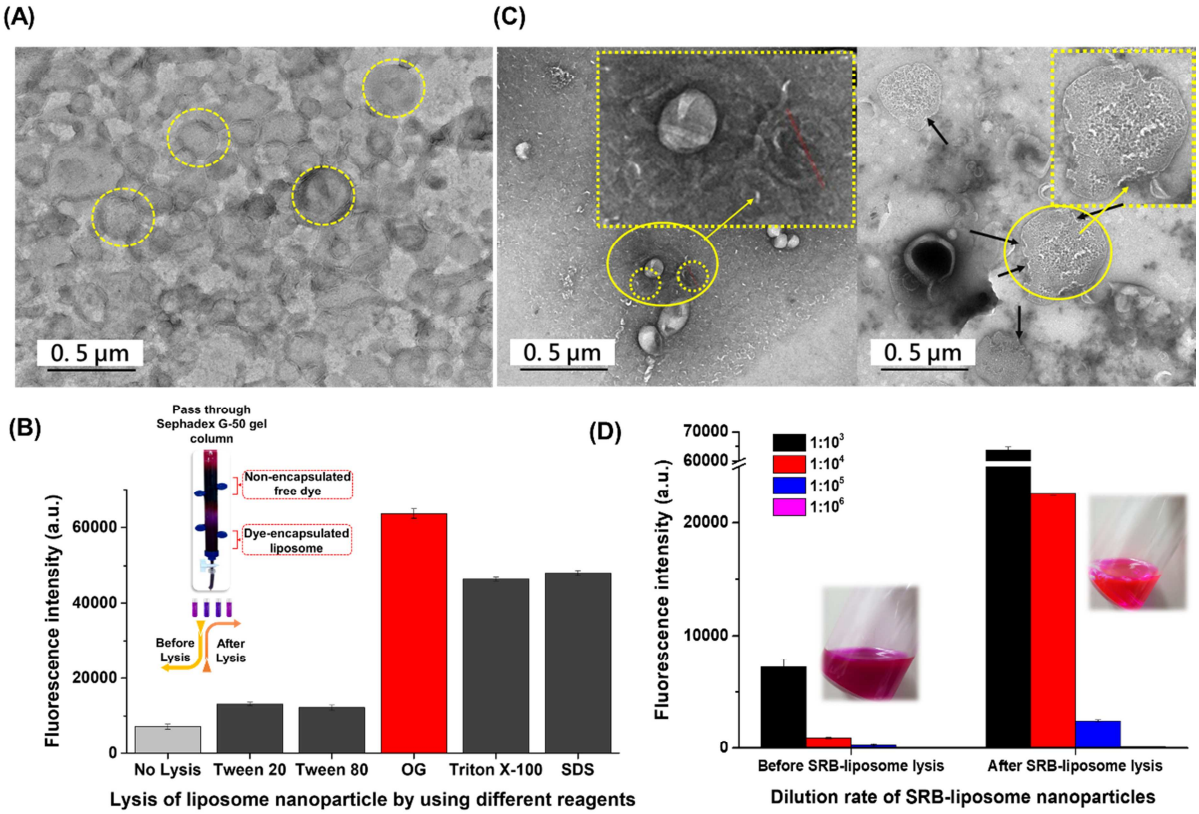
(A)
(C)
0. 5 μm
0. 5 μm
0. 5 μm
(B)
Pass through Sephadex G-50 gel column
Non-encapsulated free dye
Dye-encapsulated liposome
Before Lysis
After Lysis
Fluorescence intensity (a.u.)
0
20000
40000
60000
No Lysis
Tween 20
Tween 80
OG
Triton X-100
SDS
Lysis of liposome nanoparticle by using different reagents
(D)
Fluorescence intensity (a.u.)
70000
60000
20000
10000
0
1:10^3
1:10^4
1:10^5
1:10^6
Before SRB-liposome lysis
After SRB-liposome lysis
Dilution rate of SRB-liposome nanoparticles

Fig. 3.

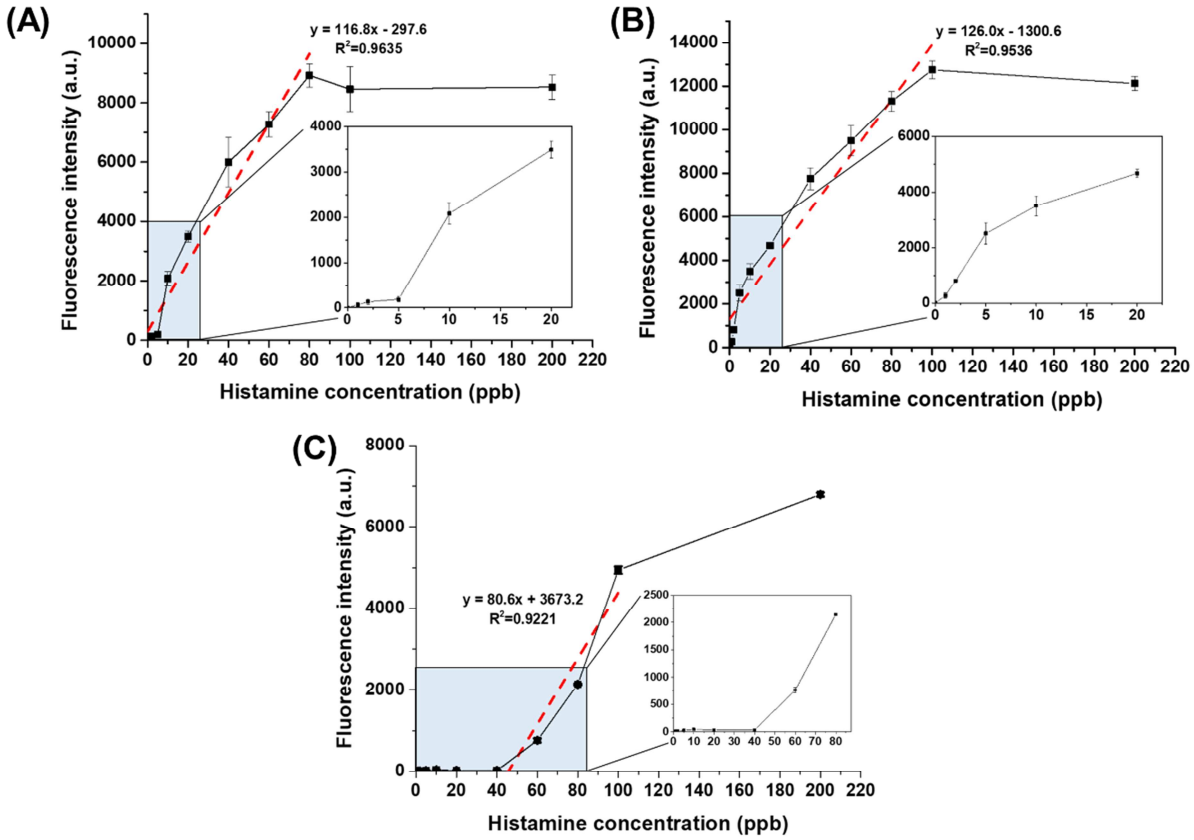

Fig. 4.

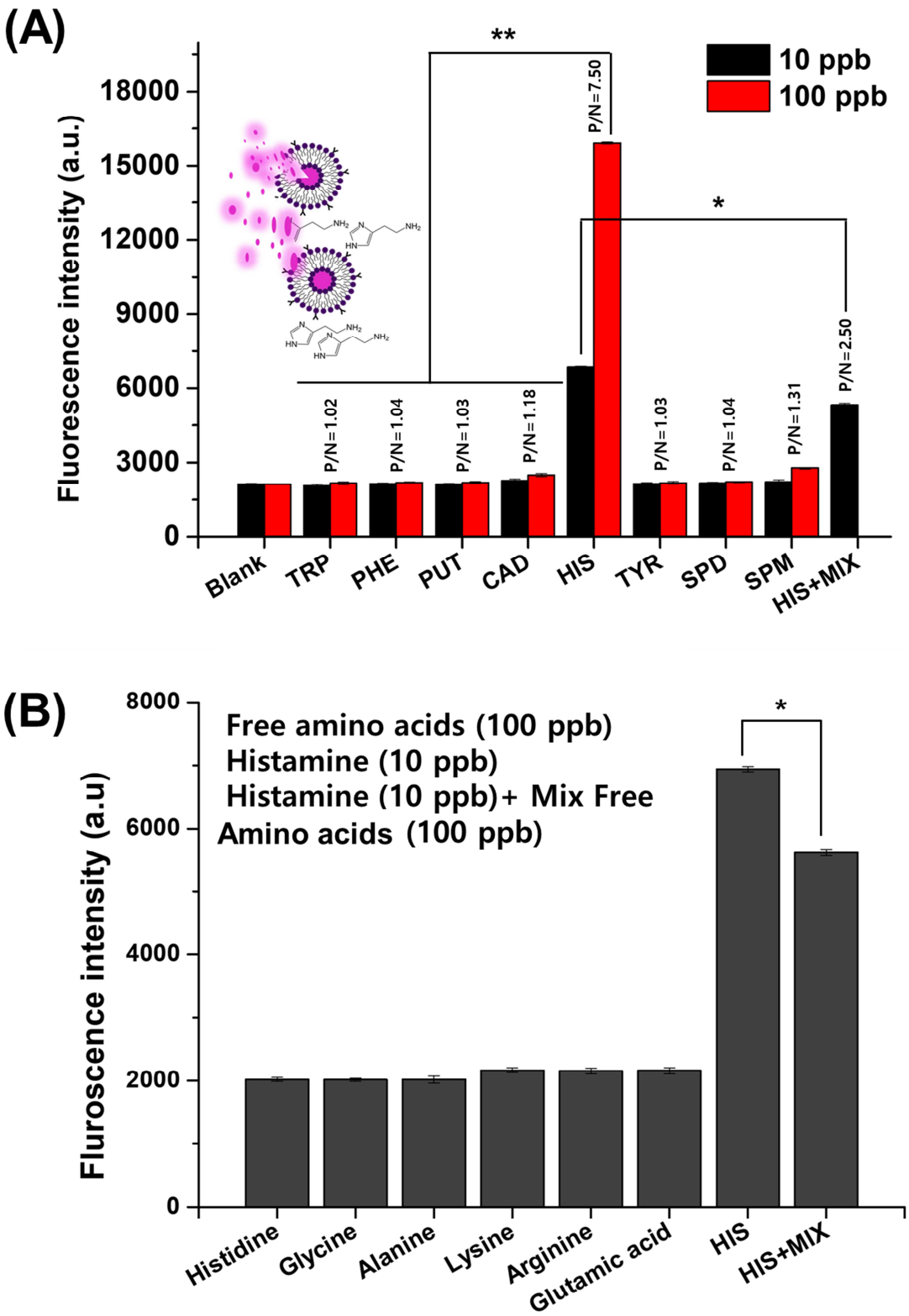
(A)
Fluorescence intensity (a.u.)
18000
15000
12000
9000
6000
3000
0
10 ppb
100 ppb
**
*
P/N=7.50
P/N=1.02
P/N=1.04
P/N=1.03
P/N=1.18
P/N=1.03
P/N=1.04
P/N=1.31
P/N=2.50
Blank
TRP
PHE
PUT
CAD
HIS
TYR
SPD
SPM
HIS+MIX
(B)
Fluroscence intensity (a.u)
8000
6000
4000
2000
0
Free amino acids (100 ppb)
Histamine (10 ppb)
Histamine (10 ppb)+ Mix Free
Amino acids (100 ppb)
*
Histidine
Glycine
Alanine
Lysine
Arginine
Glutamic acid
HIS
HIS+MIX

Fig. 5.

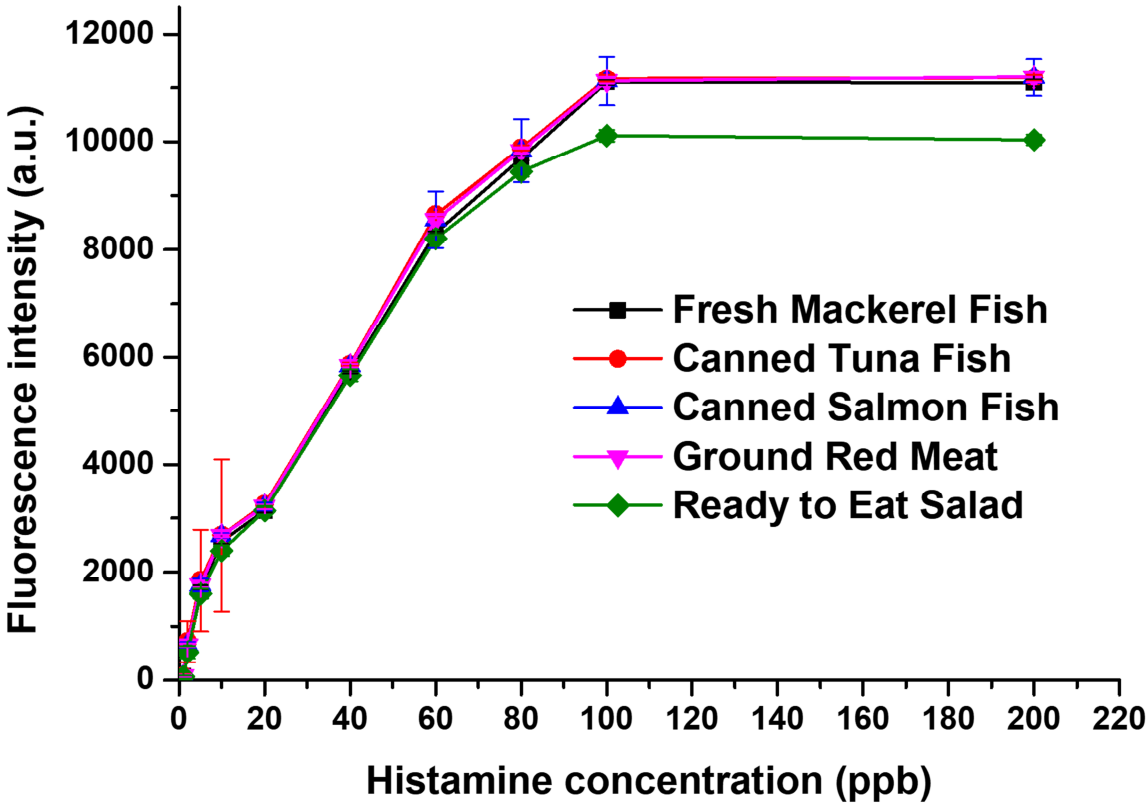

Fig. 6.

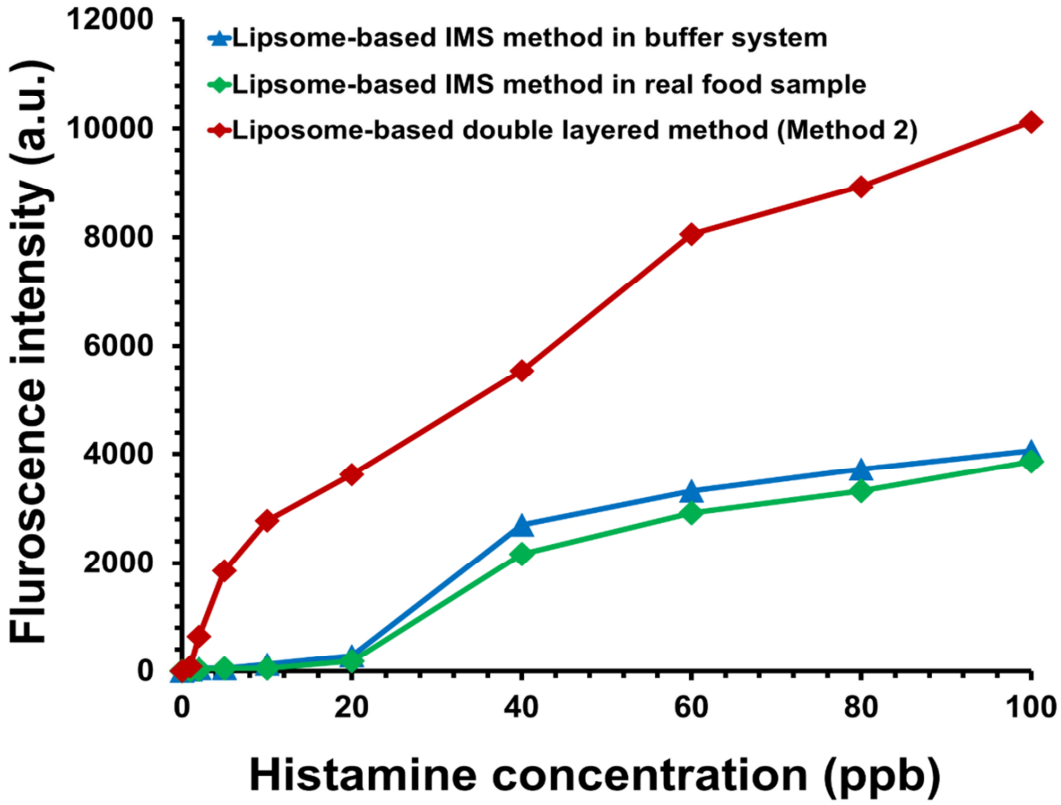

Fig. 7.

Highlights

- Scombroid fish poisoning has raised concerns due to histamine related environmental toxicity
- Double layered positioned liposomal vesicles as fluorescent probe
- Anti-histamine IgG conjugated liposomal nanovesicles (anti-His-LNs)-based multiplexed biosensing system
- Anti-His-LNs-assisted rapid, sensitive and cost-effective detection of histamine toxic molecule in fish foods
- Designed sensing platform diverse the application of various ELISA-based complicated commercial detection kits

Author contributions

The manuscript was written through contributions of all authors. All authors have given approval to the final version of the manuscript.

Declaration of interests

☒ The authors declare that they have no known competing financial interests or personal relationships that could have appeared to influence the work reported in this paper.

☐The authors declare the following financial interests/personal relationships which may be considered as potential competing interests:

Not Applicable

Yun Suk Huh, Ph.D.

Inha Fellow Professor (IFP) / Associate Professor

Inha University, Incheon, Republic of Korea

E-mail. yunsuk.huh@inha.ac.kr